Aerosol and Air Quality Research, 13: 1598–1607, 2013

ISSN: 1680-8584 print / 2071-1409 online
doi: 10.4209/aaqr.2012.10.0274

Urban Boundary Layer Height Characteristics and Relationship with Particulate Matter Mass Concentrations in Xi'an, Central China

Chuanli Du[1], Shuyan Liu[2*], Xing Yu[1], Xingmin Li[1], Chuang Chen[1], Yang Peng[1], Yan Dong[1], Zipeng Dong[1], Fanqiang Wang[1]

[1] *Meteorological Institute of Shaanxi Province, Xi'an 710015, China*
[2] *Earth System Science Interdisciplinary Center, University of Maryland, MD 20740, USA*

ABSTRACT

The characteristics of the planetary boundary layer height (PBLH) and the relationship between PBLH and particular matter (PM) mass concentration in Xi'an, central China, are analyzed in this study. Three PBLH calculation methods are used in this study, namely the Holzworth, Liu, and Nozaki approaches. The daily minimum and maximum PBLHs are determined by the Holzworth method, the hourly PBLHs are calculated by the Nozaki method, and the results of the Nozaki method are evaluated by the Liu method. The PBLH characteristics of annual, seasonal, daily, and diurnal variations are based on hourly values obtained from the Nozaki method. The results show that the Nozaki method can depict typical PBLH diurnal variations, although it substantially overestimates the related values. The daily maximum PBLH occurs from 11:00 to 16:00 Beijing time, and the seasonal maximum PBLH is during spring, due to the annual maximum wind speed at this time. $PM_{2.5}$, $PM_{1.0}$ and PM_{10} mass concentrations are negatively correlated with PBLH on the inter-annual, annual, and seasonal time scales. The anti-phase diurnal variations of PM mass concentrations and PBLH further indicate that PBLH is one of the important factors affecting air quality. The $PM_{2.5}$ in PM_{10}, $PM_{1.0}$ in $PM_{2.5}$, and $PM_{1.0}$ in PM_{10} contents show notable monthly variations, indicating that the air quality in Xi'an city is affected upwind windy and dusty weather, along with local pollution sources.

Keywords: Air quality; Mixing height; Planetary boundary layer; Particulate matter concentration; Urban boundary layer.

INTRODUCTION

Human health is strongly and consistently affected by outdoor fine particle matter, an increase of 50 μm/m^3 in the concentration causes 1–8% more increase of deaths (Wallace, 2000). Dispersion and transport of lower atmospheric pollutant depend largely on the local planetary boundary layer (PBL) structure. Turbulence process is the dominant mechanism mixing particulate matter (PM) and ambient air, the maximum well mixed height is the planetary boundary layer height (PBLH). By acting as a lid to the pollution vertical mixing extent, PBLH is one of the important factors affecting pollution concentration and large scale transport (Coulter, 1979). Thus, PBLH has been used as a key length scale in weather, climate, and air quality models to determine turbulence mixing, vertical diffusion, convective transport, cloud/aerosol entrainment, and atmospheric pollutant deposition (Deardorff, 1972; Arakawa and Schubert, 1974; Suarez *et al.*, 1983; Wesely *et al.*, 1985; Holtslag and Nieuwstadt, 1986; Stevens, 2002; Seibert *et al.*, 2000; Konor *et al.*, 2009). As one of the critical physical parameters in atmospheric environmental evaluation, studying PBLH's association with ground level PM mass concentration thus is very important for air pollution and environment quality monitoring.

The PBLH can be retrieved from observations of remote sounding systems such as lidar (Hennemuth and Lammert, 2006; Tucker *et al.*, 2009), sodar (Beyrich, 1997; Lokoshchenko, 2002), wind profiler (Angevine *et al.*, 1994; Bianco and Wilczak, 2002), ceilometer (Eresmaa *et al.* 2006; van der Kamp and McKendry, 2010), satellite (Jordan *et al.*, 2010; Ratnam and Basha, 2010). Such instrument can provide continuous measurements which is perfect for environmental quality monitoring purpose, but none of them are routinely operated and data availability are very limited. Liu and Liang (2010) developed an objective algorithm calculating PBLH from high-resolution radiosonde data. But routine operational radiosonde data are only available twice a day at 00:00 and 12:00 UTC (08:00 and 20:00 Beijing Time, hereafter) which are typically morning and evening PBL transition period (Angevine, 2008) and is insufficient to depict PBL diurnal evolution. Besides,

* Corresponding author.
Tel.: 1-301-405-1522; Fax: 1-301-405-8468
E-mail address: liusy@umd.edu

environmental evaluation and comparison needs a consistent criterion at various locations and times across the country. This highlights the importance of applying consistent algorithm for PBLH estimation which the required input data can be easily obtained at majority of the meteorological observatories.

Based on routine meteorological observations, Holzworth (1967) developed the parcel method. It determines PBLH as the equilibrium level of a hypothetical rising parcel of air representing a thermal. Holzworth method is useful for estimating daily maximum and minimum PBLHs. Nozaki (1973) developed another widely used empirical method for PBLH estimation when sounding data are unavailable. The method based on the theory that atmosphere mixed layer is the result of thermodynamic and dynamic turbulences, there exist interaction and feedback between surface meteorological variables and the atmospheric state above. Though relies only on surface observations, Nozaki method is useful for estimates of the detailed PBLH diurnal cycle and applicable to areas where radiosonde data are lacking. Cheng *et al*. (2001) used a modified Nozaki method to estimate atmospheric mixing height at Beijing Airport. The combination of PBLHs from Holzworth and Nozaki method thus provide a valuable dataset for air pollution potential prediction.

With air pollution becoming more and more severe problem in most of the cities in China, effects of PBLH on ground level PM based on in situ observational data has been studied, such as Urumqi in northwest China (Yang *et al.*, 2011), Beijing (Guo *et al.*, 2011), Chongqing in southwest China (Ye *et al.*, 2008). These studies found that PBLH is anti-correlated with PM mass concentration or air quality index of the studied city. As the capital city of Shaanxi, Xi'an is developing extremely rapid and is experiencing severe air pollution problem (Li *et al.*, 2005). Based on one year sounding data at Xi'an airport, Shi *et al*. (1997) calculated PBLH by three different methods. With the rapid development of unified design between the city and the countryside during the last several decades in China, Xi'an city expands rapidly with remarkable growing population and motor vehicles. These trends cause increasing severity of urban air pollution. Boundary layer pollution meteorological condition is one of the critical factors affecting urban air pollution (Shi *et al.*, 1997; Stull, 1988). Study PBLH characteristics and its relationship with PM mass concentration in Xi'an is of practical importance.

DATA AND METHODS

Observational Data

Data used in this study include routine surface meteorological data, sounding data, and PM mass concentration data during 2007–2009 observed at Jinghe meteorological observatory (34.43°N, 108.96°E, 411 m above sea level) in Xi'an. The observatory is located on a small hill surrounding by open land without evident pollution sources nearby, it represents the atmospheric environment of Xi'an city.

Surface routine meteorological data include precipitation, surface air temperature, wind speed and direction, cloudiness (low level and total cloudiness), and relative humidity at 1-hour interval. The sounding data are a combination of L-band radar and Balloon-Borne Sounding System. The L-band radar observes three times a day providing wind speed and direction data. The balloon typically released twice daily at 08:00 and 20:00. The observed raw data from both systems are first processed to 10 m constant vertical interval then combined to the sounding dataset including temperature, relatively humidity, wind direction, and wind speed. There is an intensive observation period during which balloon was also released at 14:00 from May 18 to 24, 2008. The observations during this period will be used to evaluate Nozaki method.

The PM mass concentration was observed by GRIMM 180 Dust Monitor manufactured by GRIMM Aerosol Company in Germany. The Dust Monitor uses light-scattering technology for atmospheric particle counts and diameter ranges according to the frequency and intensity of the scatted laser beam by the particles. Particle mass concentration for PM_{10} (Particulate Matter less than 10 μm), $PM_{2.5}$ (Particulate Matter less than 2.5 μm), $PM_{1.0}$ (Particulate Matter less than 1.0 μm) then calculated under the assumption of spherical particle. The temporal interval of the GRIMM 180 at Jinghe observatory is 5 minutes. The data are processed to 1-hour interval in this study.

PBLH Calculation Methods

Three PBLH determination methods are used in this study. Liu method (Liu and Liang, 2010) which is based on potential temperature profile will be used to evaluate Nozaki method at sounding times (08:00, 14:00, and 20:00). The boundary layer stability is first classified by potential temperature profile as follows:

$$\theta_5 - \theta_2 \begin{cases} < -1.0 & \text{unstable} \\ > +1.0 & \text{stable} \\ \text{else} & \text{neutral} \end{cases} \quad (1)$$

where θ is potential temperature (K) and its subscript number is the level index starting from surface.

For unstable boundary layer, due to the dominant role of buoyancy driving the turbulence, the PBLH is determined as the height at which an air parcel rising adiabatically from the surface becomes neutrally buoyant (Stull, 1988). Neutral boundary layer height is calculated by the same procedure. For stable boundary layer, the PBLH is defined as the transition from a stable to a neutral or unstable condition above. According to this definition, the method determines stable PBLH as the first level at which θ gradient reaches minimum and there is no adjacent temperature inversion layer above (Liu and Liang, 2010).

Fig. 1 presents PBLH under the three stability classes calculated by Liu method based on potential temperature vertical profiles. The sounding data are at 08:00 (morning), 14:00 (noon), and 20:00 (evening) during May 21, 2008. Fig. 1 shows that the PBLH is 424 m in the morning with distinct residual layer from previous daytime well mixed layer, increased to 827 m in the noon due to surface

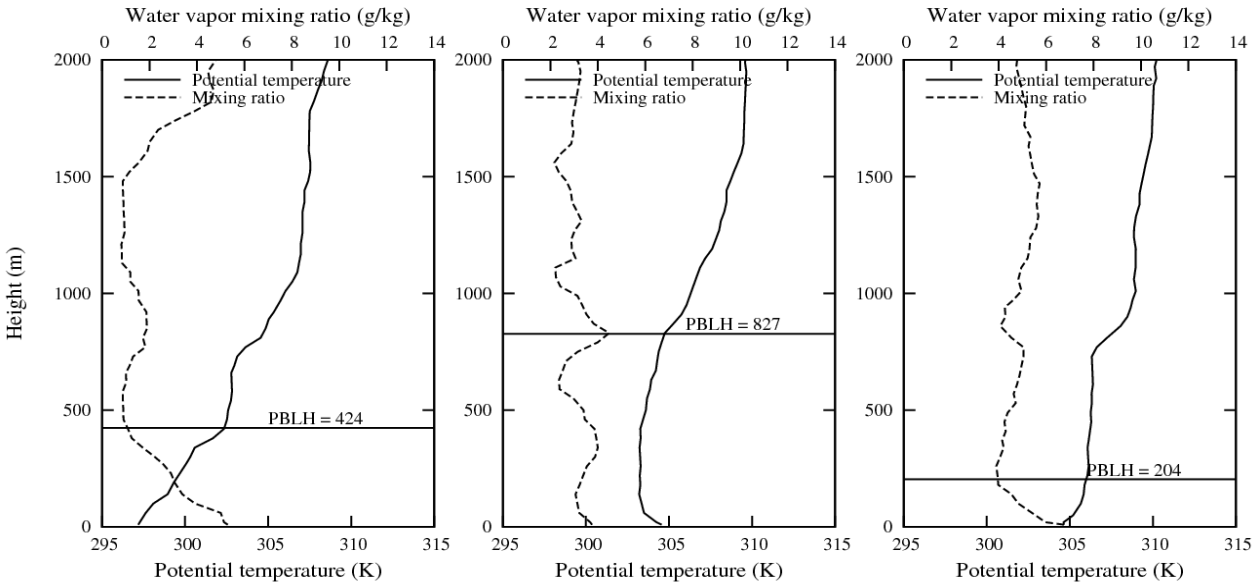

Fig. 1. PBLH (m) calculated by Liu method based on potential temperature profile at 08:00 (a), 14:00 (b) and 20:00 (c) Beijing Standard Time during May 21, 2008.

temperature rise and active convective development, potential temperature and water vapor are well mixed in the PBL; at night, with surface cooling and temperature decreasing, higher level atmospheric temperature change lagged behind the near surface temperature which result in aloft temperature inversion, the PBLH is defined at the temperature inversion top (204 m). Liu method realistically determined PBLH for morning stable, noon convective unstable and early evening near neural boundary layer stability classes. Liu and Liang (2010) demonstrate that Liu method is a useful algorithm for faithful PBLH calculation. The results justified its evaluation role for Nozaki method.

The Nozaki empirical PBLH determination method is based on routine surface meteorological observations for various Pasquill (1961) stability classifications. Pasquill (1961) classified the atmospheric stability into six classes from A to F in terms of increasing order from very unstable (A), moderately unstable (B), slightly unstable (C), neutral (D), slightly stable (E) to moderately stable (F). The presence of class A indicates strong mixing whereas E or F gives rise to poor dispersion. Unstable conditions promote rapid dispersion of atmospheric contaminants and result in lower air concentrations compared with stable conditions. The atmospheric stability class is determined according to solar radiation calculated by solar altitude, cloud cover, and wind speed. The Nozaki PBLH calculation method is as follows:

$$H = \frac{121}{6}(6-P)(T-T_d) + \frac{0.169P(U_z+0.257)}{12f\ln(Z/z_0)} \quad (2)$$

$$f = 2\Omega\sin\varphi \quad (3)$$

where H is the PBLH, P is the Pasquill stability level, value is 1–6 for A–F stability class, T is the surface air temperature, T_d is the surface air dew-point temperature, U_z is the mean wind speed (m/s) at height of Z (Z = 10 m), f is the Coriolis parameter (s^{-1}), z_0 is the surface roughness length (0.5 m in this study), Ω is the (7.29×10^{-5} rad/s), φ is the latitude. T, T_d, and P are factors considering thermodynamic mechanism, while U_z and z_0 are taking turbulence and dynamic mechanisms into account.

Holzworth (1967) method will be used to calculate daily maximum and minimum PBLH based on 08:00 and 20:00 sounding profile, respectively. The PBLH is determined as the level at which maximum or minimum surface air temperature follows the dry adiabatic lapse rate up to the intersection with the observed temperature sounding. Holzworth method was developed for urban environment in order to estimate urban air pollution which coincides with the purpose of this study.

RESULTS

PBLH Comparisons among the Three Calculation Methods

Fig. 2 is the PBLH diurnal cycle calculated by Nozaki method for the three intensive observation days (May 20, 21, and 22, 2008). Typical PBLH diurnal cycles are well-defined by Nozaki method peaked during the period of 11:00–16:00. The morning PBLH erupts at about 05:00 and evening PBLH collapse at about 20:00.

To further evaluate Nozaki method, Table 1 is the PBLH comparisons between Liu and Nozaki method at sounding times during the three intensive observation days. Nozaki method generally calculated higher PBLH than Liu method. The two methods are the same at 14:00 on May 22, 2008 (1492 m), close at 08:00 on May 20, 2008 with 207 m difference. The PBLH climatology mean at 08:00 and 20:00 during 2007–2009 (Table 3) also indicating overestimation by Nozaki method. These results are consistent with Ma and Zheng (2011) stating that Nozaki method reflects daily variations of mixing layer with overestimation of low PBLHs.

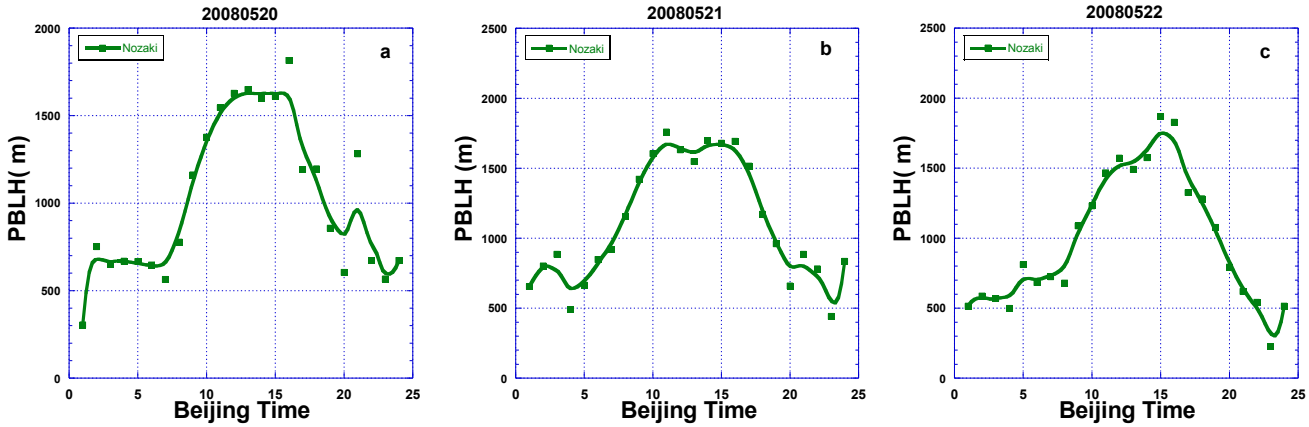

Fig. 2. PBLH (m) diurnal cycles calculated by Nozaki method for May 20 (a), 21 (b), and 22 (c), 2008.

Table 1. PBLH comparisons between Liu and Nozaki method at sounding times (08:00, 14:00, 20:00 Beijing Time) during May 20, 21, and 22, 2008.

	5/20		5/21		5/22	
	Liu	Nozaki	Liu	Nozaki	Liu	Nozaki
08:00	367.0	574.5	424.0	918.6	191.0	725.1
14:00	692.0	1648.6	827.0	1548.2	1492.0	1492.2
20:00	46.0	858.0	204.0	960.3	214.0	1077.1

Table 2 is maximum and minimum PBLH comparisons between Holzworth and Nozaki method. The maximum and minimum PBLHs calculated by the two methods agree fairly well, with the maximum PBLH differences are 375, 949, and 412 m for May 20, 21, and 22. The difference for May 21 is higher than the other two which attributing to the lower daily maximum temperature (about 2°C lower) Holzworth method relies on. The minimum PBLH differences are close during the three days with Nozaki method is higher except for May 21. The absolute values of the differences are 135, 189, and 215 m for May 20, 21, and 22. Again, May 21 has the highest daily minimum temperature resulting in higher Holzworth PBLH. Previous studies showed that PBLH based on radiosonde and lidar data typically deviates ± 200 m (Hennemuth and Lammert, 2006; Liu and Liang, 2010) for daytime convective boundary layer, and PBLH based on radiosonde and sodar data deviates ± 167 m (Liu and Liang, 2010). Thus, the differences between Holzworth and Nozaki method are within the acceptable range.

Table 3 is the climatology averaged PBLH during 2007–2009. Note that the minimum PBLH based on Nozaki method is the daily minimum among the 24 values and not necessarily occurs at the same hour each day. Maximum PBLH are in well agreement with acceptable differences (185, 143, 59.2, 224.7, and 343.9 for annual, spring, summer, fall, and winter) between Holzworth and Nozaki method. Large discrepancies exist for minimum PBLH, Holzworth PBLH are all below 100 m. In contrast, Nozaki minimum PBLH are several hundred meters and can as high as 701.8 m in spring.

Though Nozaki method shows certain differences from Liu method at 08:00 and 20:00 (Table 3), the PBLH diurnal cycle is well constructed (Fig. 2). Along with its required data always available at hourly temporal interval which is essential for diurnal variation analyis, , Nozaki method is a simple and easy to apply as well as useful method for PBLH characteristics analysis, and for the study of PBLH and PM mass concentration relationship which are very useful for air pollution potential prediction. Since Holzworth method uses the vertical profile of atmospheric states and surface temperatures (minimum and maximum) in contrast to that Nozaki method only uses surface data, minimum and maximum PBLH determined from Holzworth method will be sued in the following analysis.

PBLH Statistical Characteristics

To facilitate statistical analysis, the six Pasquill stability classifications are further divided to the following three classes, unstable class includes A, B, and C, neutral class includes D, and stable class includes E and F. Fig. 3 shows

Table 2. Maximum and minimum PBLHs comparisons between Holzworth and Nozaki method during May 20, 21, and 22, 2008.

	5/20		5/21		5/22	
	Holzworth	Nozaki	Holzworth	Nozaki	Holzworth	Nozaki
Max_PBLH (m)	1440.0	1814.9	810.0	1759.0	2280.0	1868.4
Min_PBLH (m)	170.0	304.5	630.0	441.0	510.0	725.1

Table 3. PBLH comparisons between different methods during 2007–2009.

	Annual		Spring		Summer		Fall		Winter	
	Holzworth	Nozaki	Holzworth	Nozaki	Holzworth	Nozaki	Holzworth	Nozaki	Holzworth	Nozaki
Max_PBLH	1062.7	1247.7	1366.4	1509.4	1221.8	1281.0	820.2	1044.9	840.9	1184.8
Min_PBLH	68.44	619.61	69.3	701.79	89.5	630.35	55.6	527.01	59.3	265.71
	Liu	Nozaki	Liu	Nozaki	Liu	Nozaki	Liu	Nozaki	Liu	Nozaki
08:00	232.07	621.98	231.95	706.98	231.22	657.32	228.13	521.25	236.80	602.13
20:00	292.83	802.95	248.33	941.02	441.24	948.25	204.53	662.67	273.23	658.24

the stability classes frequency distribution based on 1089 sounding data during 2007–2009. The unstable class start to appear at 07:00 in the morning (4.1%), reached the maximum at 14:00 (78.9%), then decreased at 18 (11.1%). The stable class appears at 17:00 (11.4%), reached the maximum at 00:00 (80.89%), and disappeared from 09:00 (6.5%). The neutral class observed during the whole day with two distinct peaks at 08:00 and 17:00 in the morning and afternoon, respectively.

Fig. 4 is the frequency distribution of PBLH calculated by Nozaki method under the three stability conditions. They are calculated for bins of every 50m PBLH interval, from 25–75 m to 2975–3025 m.

The PBLH frequency distributions differ significantly between the stable, neutral and unstable regimes. The stable boundary layer frequency follows well a narrow distribution ranging from 25 to 1500 m with most frequency at 500 m (about 1000 samples). In contrast, the convective boundary layer frequency is depicted by a broad distribution which has a quite flat shape with a wider PBLH range from 100 to 3000 m peaks at 1000 m (about 300 samples). The peak occurrence drops substantially from 1000 samples for stable class to 300 samples unstable class. The neutral frequency is intermediate of the two and close to unstable class ranging from 25 to 2350 m and peaks at 800 m (about 400 samples).

Fig. 5 is the mean PBLH diurnal variations during 2007–2009 calculated by Nozaki method for annual, spring (March–April–May), summer (June–Jul–August), fall (September–October–November) and winter (December–January–February). PBLH is about 600 m during nocturnal stable boundary layer, rises gradually from 08:00 in the morning, reaches the maximum of over 1000 m at 16:00, then decreases gradually to nocturnal average height at 21:00. The seasonal diurnal cycles coincide with the annual average diurnal variations. The seasonal maximum diurnal PBLH ordering from highest to lowest are spring, summer, winter and fall with the height of 1509.4, 1248.9, 1184.8, and 1044.9 m, respectively.

Relationship between PM Mass Concentration and PBLH

Fig. 6(a) is the PBLH daily averaged PBLH during January 1, 2007 to December 31, 2009. The daily mean PBLHs are based on Nozaki method, daily maximum and minimum PBLHs are calculated from Holzworth method. The daily averaged PBLH shows clear annual cycle with the minimum height during winter in January every year, reaches maximum in May to about 1500 m, then decreases to about 1000 m July, and further decreases in fall. The

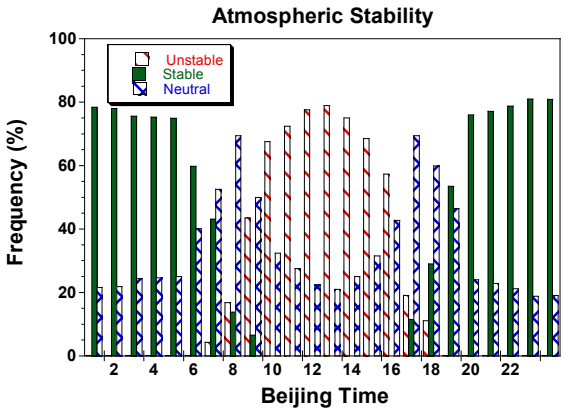

Fig. 3. Diurnal distribution of atmospheric stability frequencies (%) for unstable, stable, and neutral classes during 2007–2009.

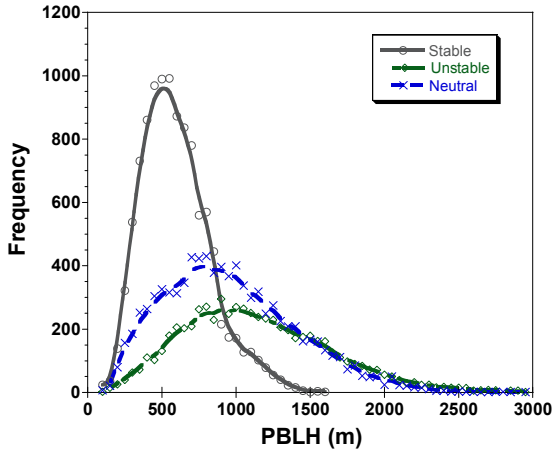

Fig. 4. PBLH frequency distributions under unstable, stable, and neutral classes for bins of every 50 m interval calculated by Nozaki method.

PBLH daily maximum variation is very similar to that of the daily average, which also shows clear annual cycle peaking during spring in May and the valley is during winter in January. The scatter points show that the maximum PBLH can reach as high as 3000 m during summer. The inter-annual variations of daily minimum is different from that of daily average and daily maximum without a clear annual cycle, and the trend line is around 100 m.

Fig. 6(b) is the variations of the daily average PM concentrations. Since GRIMM180 is not a routine meteorological observation instrument, there is no substitute

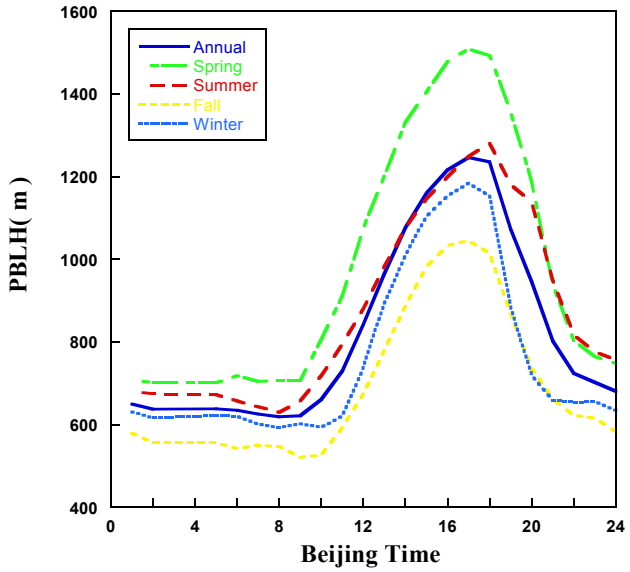

Fig. 5. Diurnal variations of PBLH (m) annual and seasonal mean during 2007–2009 calculated by Nozaki method.

instrument if it encountered any problems during operation or during maintenance which resulted in long time no-data period (white space in the figure), while this situation improved after 2009. The variations of PM_{10}, $PM_{2.5}$, and $PM_{1.0}$ concentrations are following each other with concentration ranges between 50–350, 40–250, and 30–200 $\mu g/m^3$, respectively. All three PM concentrations are reach maximum during winter, minimum during spring, summer, and fall are in between. PM_{10} shows notable higher concentration during spring than during fall. Xi'an locates to the east of Loess Plateau and dust frequently occurs during spring (Ning *et al.*, 2005) which explained the higher PM_{10} concentration during spring. Comparison between Figs. 6(a) and 6(b) indicates PBLH anti-correlates with PM concentration, higher PBLH corresponds to lower PM concentration and vice versa.

Table 4 shows statistical results between PBLHs and PMs. All the correlation coefficients are negative indicating anti-relationship which is in agreement with Fig. 6. $PM_{2.5}$ and $PM_{1.0}$ are significantly ($P < 0.001$) negatively correlated with daily average and maximum PBLH. PM_{10} is more

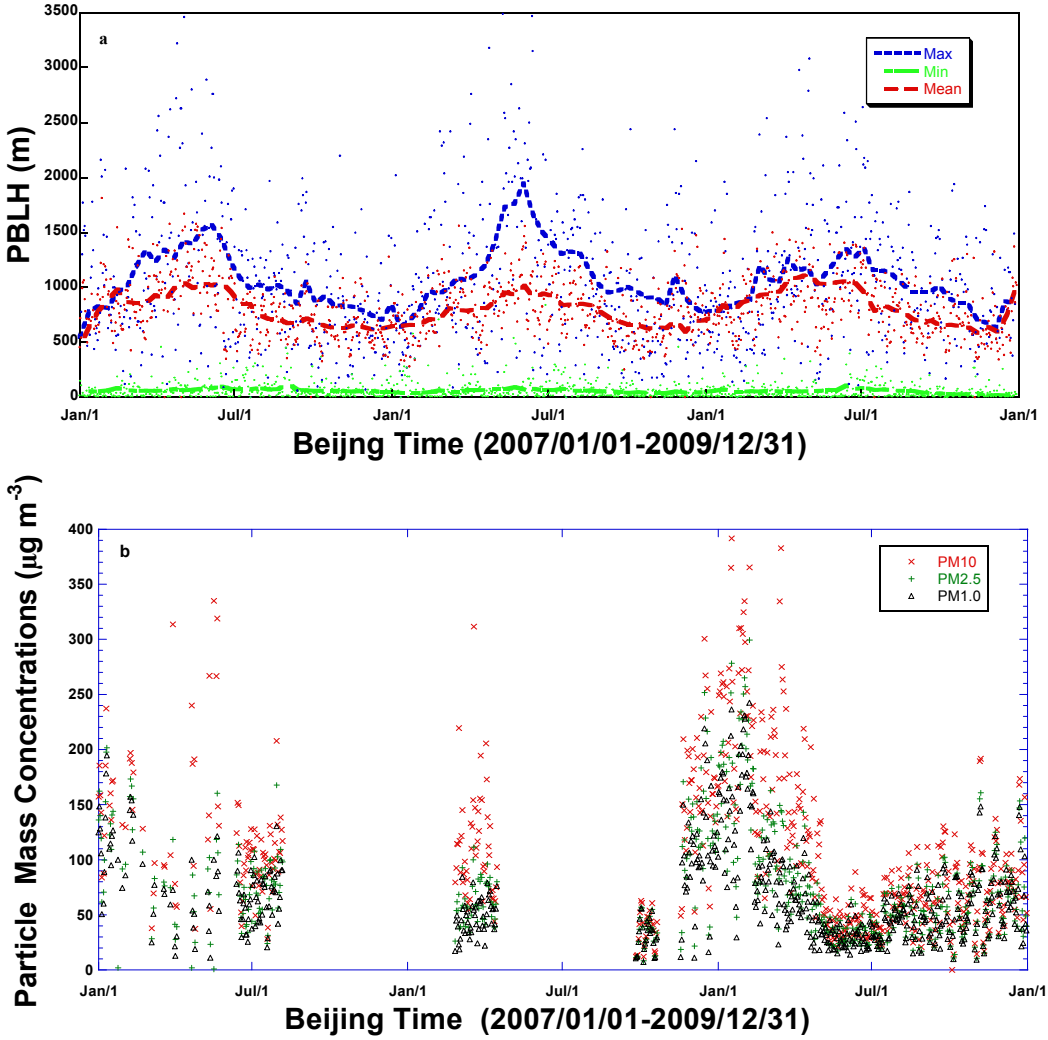

Fig. 6. Daily average variations of PBLH (a, unit: m) and PM mass concentrations (b, unit: $\mu g/m^3$) during 2007–2009. The mean value is based on Nozaki method, the minimum and maximum value are based on Holzworth method.

affected by daily maximum PBLH. Daily minimum PBLH does not show significant (P > 0.001) effects on all three PM concentrations.

Monthly mean values of PBLH and three PM concentrations are calculated to further analyze their relationship. Fig. 7 is the monthly variations for PBLH and three PM concentrations which shows evident anti-correlation between them. Concentrations of three PMs decrease rapidly from January, reached minimum during May, June, and July, then increase gradually from August till December. PBLH variations are opposite which increase gradually from January, reaches maximum during June and July, then decrease gradually from August till December. The opposite phase indicates that PBLH determined the height that atmospheric pollution can disperse. Under the circumstance of constant pollution sources, pollutant accumulates gradually inside the PBL and cause concentration increase if there is no upper reaches weather systems' intervene. Thus, clarify the relationship between PBL structure and atmospheric PM concentration will facilitate not only the analysis of pollutant variations, but also provide basis studies for monitor and forecast urban atmospheric environment.

Fig. 8 is the diurnal cycle of PBLH and PM mass concentrations during 2007–2009. Please note that the PBLH annual diurnal cycle is the same as in Fig. 5. The PM mass concentrations typically show higher value during nighttime when PBLH is relatively low, while lower value during daytime. The diurnal lowest value for all the three PMs occur at 17:00 which corresponding to PBLH peak. The anti-phase variation between PBLH and PMs further indicates that shallow PBL typically favors pollutant built-up and thus worse air quality, while deep PBL related to better air quality.

The PBLH is affected by many factors such as temperature, sensible and latent heat fluxes, cloud cover, relative humidity, wind speed, etc. Generally, winter has the minimum PBLH, spring and fall is higher, and summer has the maximum height (Shi *et al.*, 1997; Liu and Liang, 2010). Fig. 7 shows notably higher PBLH in spring than in fall which mainly due to the stronger wind during spring in Xi'an. To illustrate this reason, the monthly mean wind speed is calculated based on daily wind speed data during the same period, the results are showed in Fig. 9. The mean wind speed during spring seasons is remarkably stronger than during the fall and winter, close to the speed during summer. The wind speed during spring is 3.0 m/s, while during fall is only 2.4 m/s. This difference partially explained the higher spring PBLH than fall and winter.

Concentrations of the pollutant are not constant through the year, its component variations indicate that these pollutants are not only affected by the local source, but also remote sources in other locations. Fig. 10 is the monthly mean variations of concentrations of $PM_{2.5}$, $PM_{1.0}$, $PM_{1.0}$ in PM_{10}, $PM_{2.5}$, PM_{10}, respectively. The three lines show very

Table 4. Correlation coefficients between daily PBLH (average, maximum, and minimum) and PM_{10}, $PM_{2.5}$ and $PM_{1.0}$ during 2007–2009.

	Avg_PBLH	Max_PBLH	Min_PBLH
PM_{10}	–0.095 (P = 0.055)	–0.151 (P = 0.003)	–0.118 (P = 0.017)
$PM_{2.5}$	–0.249 (P < 0.001)	–0.247 (P < 0.001)	–0.119 (P = 0.015)
$PM_{1.0}$	–0.321 (P < 0.001)	–0.281 (P < 0.001)	–0.118 (P = 0.017)

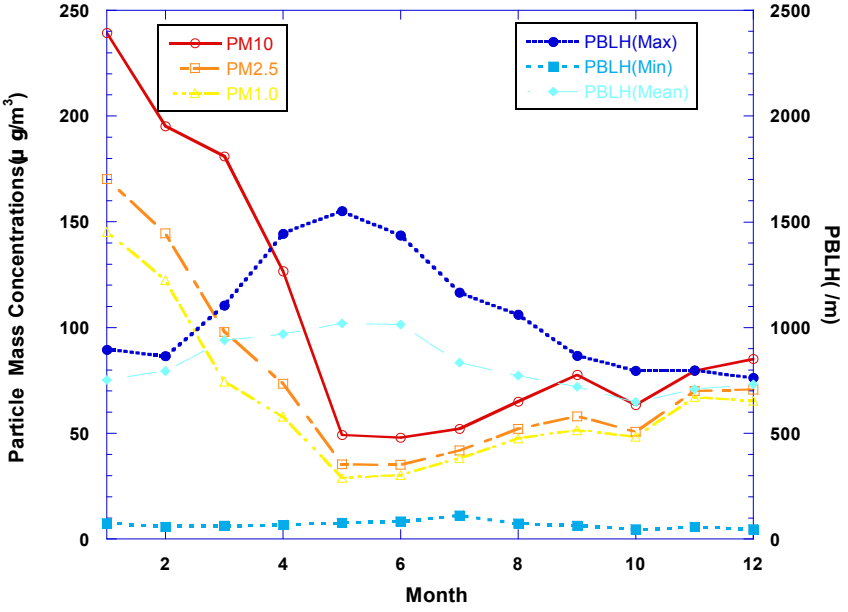

Fig. 7. Monthly average variations of PBLH (scale on right, unit: m) and PM mass concentrations (scale on left, unit: μg/m^3) during 2007–2009.

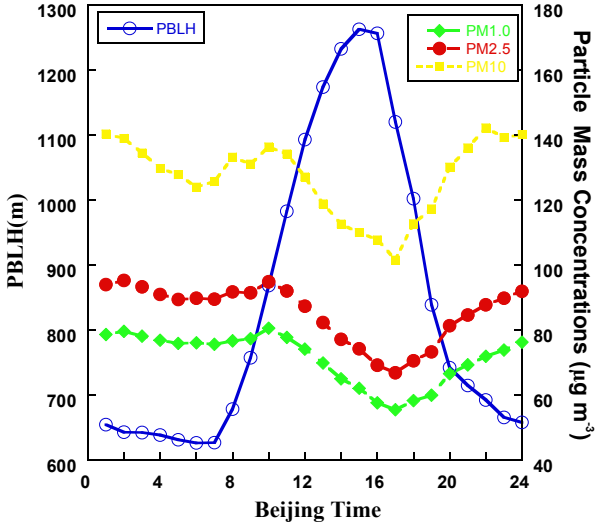

Fig. 8. Diuranl variations of PBLH (scale on right, unit: m) and PM mass concentrations (scale on left, unit: μg/m^3) during 2007–2009.

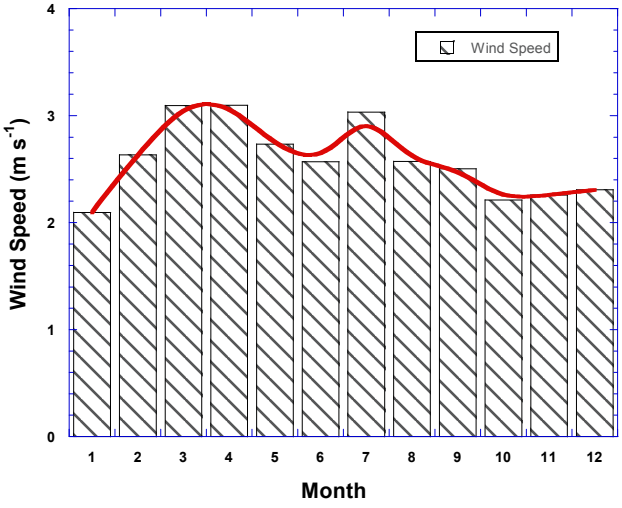

Fig. 9. Monthly variations of wind speed (unit: m/s) during 2007–2009.

similar variation trend. Concentration percent of $PM_{2.5}$ in PM_{10} ranges between 55%–90% with the minimum and maximum values during March and November, and the average percentage is 74%. Concentration content percent of $PM_{1.0}$ in $PM_{2.5}$ is between 75%–95%, the minimum and maximum values also during March and November with the average value of 87%; Concentration percent of $PM_{1.0}$ in PM_{10} is between 40%–85% with the same minimum and maximum months (March and November) as the other two, the average value is 65%.

The $PM_{2.5}$ is the main component of Xi'an urban atmospheric pollutant which is 74% in average in PM_{10}. While, the percentage of $PM_{1.0}$ in $PM_{2.5}$ ranges from 75%–90% and the average value is 87%. The above results indicate that the main pollutants are small particles from anthropogenic sources which include motor vehicle emission, residential emission, power plant, and architectural floating dust pollution, etc. All three curves in Fig. 10 are notably low during March and April. The main reason is that windy and dusty weather occurs frequently during spring in Xi'an result in dusk percentage in particle concentration is higher than during the other seasons. With local pollutant sources constant, larger denominator cause lower percentage of $PM_{2.5}$, $PM_{1.0}$ in. The decreased percentage of $PM_{1.0}$ in $PM_{2.5}$ also noticed during March and April with less degree.

CONCLUSION AND DISCUSSION

Xi'an located at the center of Kuan-chung Plain with mountains to both the south and north. This special geographical characteristic resulted in Xi'an's atmospheric environmental quality not to be optimistic. The paper uses multiple datasets from sounding, surface meteorology, automatic, and atmospheric component stations, applies three different methods to calculated urban PBLH, and analyzes its effects on the fine PM concentration.

Nozaki method captures the typical PBLH characteristics such as diurnal cycle with overestimation for nocturnal stable boundary layer. Nozaki method produces very close maximum PBLH with Holzworth method, while higher minimum PBLH. Based on Pasquill stability classification, stable boundary layer occurs during 17:00 to 09:00 mainly at night, unstable boundary layer happens during 07:00 to 17:00 with the majority at noon, neutral boundary layer shows all day long and double peaks at 08:00 and 18:00 which are morning and evening transition period. Probability frequency distribution for unstable, neutral and stable PBLH based on Nozaki method showed that the most occurrence height for stable class is 500 m, for neutral class is 800 m, and for unstable class is 1000 m. The annual and seasonal mean diurnal variations follow each other peaking at 1600 with high to low order is spring, summer, winter, and fall, annual average is very close to that of summer.

PM concentrations are inversely correlated with daily maximum (Holzworth method) and mean (Nozaki method) PBLH, $PM_{2.5}$ and $PM_{1.0}$ are statistically significant during 2007–2009. Monthly mean PM_{10}, $PM_{2.5}$, $PM_{1.0}$ during the same period also show reversed variation with monthly mean maximum and average PBLH. The anti-phase diurnal variations of PM mass concentrations and PBLH further indicates that PBLH is one of the important factors affecting air quality. Shallow PBLH typically corresponds to higher PM mass concentrations, while deep PBLH corresponds to lower mass concentrations.

Annual maximum wind speed occurs during spring in March and April partially explained the annual maximum PBLH and minimum PM concentrations in spring rather other seasons. Content percentage of $PM_{2.5}$ in PM_{10}, $PM_{1.0}$ in $PM_{2.5}$, and $PM_{1.0}$ in PM_{10} show distinct monthly variations with all notably low during spring of March. This indicates that besides local pollution sources, Xi'an also affected by upwind windy and dusty weather in spring which resulted in lower content during the season. This study only focused on PBLH's effects on air quality. Other than PBLH, emission is among the fundamental factors to

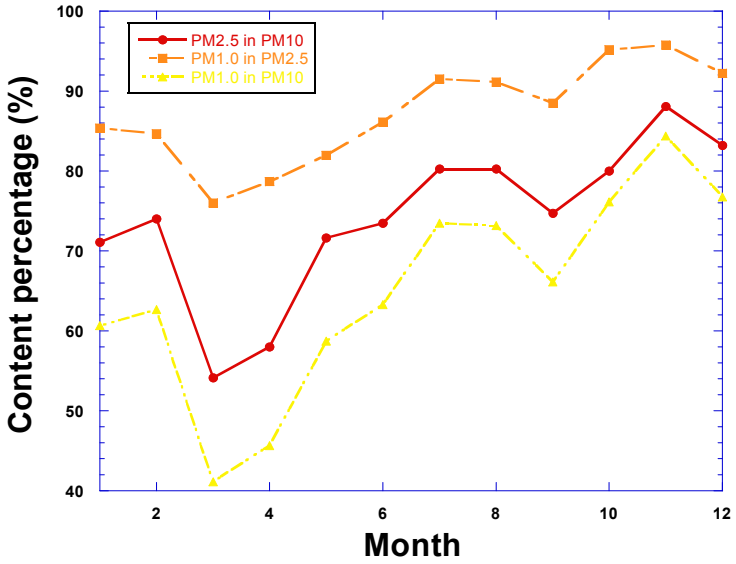

Fig. 10. Monthly variations content percentage (unit: %) of $PM_{2.5}$ in PM_{10}, $PM_{1.0}$ in $PM_{2.5}$, $PM_{1.0}$ in PM_{10} during 2007–2009.

air quality, and to some less degree, long-range transport and atmospheric chemistry. The high PM concentration during winter months may mainly due to the large emissions during the heating season. In summer, the secondary aerosol also plays a large role in contributing to overall PM.

The results of this analysis present a promising application of surface routine meteorological observations estimated PBLH in ambient air quality monitoring. Since surface observations are routinely operated, current results are valuable for other cities and areas.

ACKNOWLEDGEMENTS

The research was supported by China Special Fund for Meteorological Research in the Public Interest GYHY201306005 and the National Basic Program of China (973 Program, 2013CB955800) and the Climate Change Special Fund of China Meteorological Administration CCSF201327. The views expressed are those of the authors and do not necessarily reflect those of the sponsoring agencies and the Meteorological Institute of Shaanxi Province. We would like to thank the two anonymous reviewers for their instructive comments.

REFERENCES

Angevine, W.M., White, A.B. and Avery, S.K. (1994). Boundary Layer Depth and Entrainment Zone Characterization with a Boundary Layer Profiler. *Boundary Layer Meteorol.* 68: 375–385.

Angevine, W.M. (2008). Transitional, Entraining, Cloudy, and Coastal Boundary Layers. *Acta Geophys.* 56: 2–20.

Arakawa, A. and Schubert, W.H. (1974). Interaction of a Cumulus Cloud Ensemble with the Large-scale Environment, Part I. *J. Atmos. Sci.* 31: 674–701.

Beyrich, F. (1997). Mixing Height Estimation from Sodar Data: A Critical Discussion. *Atmos. Environ.* 31: 3941–3953.

Bianco, L. and Wilczak J.M. (2002). Convective Boundary Layer Depth: Improved Measurement by Doppler Radar Wind Profiler Using Fuzzy Logic Methods. *J. Atmos. Oceanic Technol.* 19: 1745–1758.

Cheng, S., Huang, G., Chakma, A., Hao, R., Liu, L. and Zhang, X. (2001). Estimation of Atmospheric Mixing Heights Using Data from Airport Meteorological Stations. *J. Environ. Sci. Health., Part A* 36: 521–532.

Coulter, R.L. (1979). A Comparison of Three Methods for Measuring Mixing-layer Height. *J. Appl. Meteorol.* 18: 1495–1499.

Deardorff, J.W. (1972). Parameterization of the Planetary Boundary Layer for Use in General Circulation Models. *Mon. Weather Rev.* 100: 93–106.

Eresmaa, N., Karppinen, A., Joffre, S.M., Räsäner, J. and Talvitie, H. (2006). Mixing Height Determination by Ceilometers. *Atmos. Chem. Phys*. 6: 1485–1493.

Garratt, J.R. (1992). *The Atmospheric Boundary Layer*, Cambridge University Press, New York.

Guo, L., Zang, Y., Liu, S., Li, J. and Ma, Y. (2011). Correlation Analysis between PM_{10} Mass Concentration and Meteorological Elements of Atmospheric Boundary Layer in Beijing Area. *Acta Sci. Nat. Univ. Pekin.* 47: 607–612.

Hennemuth, B. and Lammert, A. (2006). Determination of the Atmospheric Boundary Layer Height from Radiosonde and Lidar Backscatter. *Boundary Layer Meteorol.* 120: 181–200.

Holtslag, A.A.M. and Nieuwstadt, F.T.M. (1986). Scaling the Atmospheric Boundary Layer. *Boundary Layer Meteorol.* 36: 201–209.

Holzworth, G. (1967). Mixing Depths, Wind Speeds and Air Pollution Potential for Selected Locations in the United States. *J. Appl. Meteorol.* 6: 1039–1044.

Jordan, N.S., Hoff, R.M. and Bacmeister, J.T. (2010). Validation of Goddard Earth Observing System-version 5 MERRA Planetary Boundary Layer Heights Using CALIPSO. *J. Geophys. Res.* 115, doi: 10.1029/2009JD

013777.

Konor, C.S., Boezio, G.C., Mechoso, C.R. and Arakawa, A. (2009). Parameterization of PBL Processes in an Atmospheric General Circulation Model: Description and Preliminary Assessment. *Mon. Weather Rev.* 137: 1061–1082.

Li, Y., Cao, J., Zhang, X. and Che, H. (2005). The Variability and Source Apportionment of Black Carbon Aerosol in Xi'an Atmosphere during the Autumn of 2003. *Clim. Environ. Res*. 10: 229–237.

Liu, S. and Liang, X.Z. (2010). Observed Diurnal Cycle Climatology of Planetary Boundary Layer Height. *J. Clim.* 23: 5790–5809.

Lokoshchenko, M.A. (2002). Long-term Sodar Observations in Moscow and a New Approach to Potential Mixing Determination by Radiosonde Data. *J. Atmos. Oceanic Technol.* 19: 1151–1162.

Ma, J. and Zheng, X. (2011). Comparisons of Boundary Mixing Layer Depths Determined by the Empirical Calculation and Radiosonde Profiles. *J. Appl. Meteorol. Sci.* 22: 567–576.

Ning, H., Wang, S. and Du, J. (2005). Characteristics of Sand-dust Events and Their Influence on Air Quality of Xi'an City. *J. Desert Res*. 25: 886–890.

Nozaki, K.Y. (1973). *Mixing Depth Model Using Hourly Surface Observations,* Report 7053, USAF Environmental Technical Applications Center.

Pasquill, F. (1961). The Estimation of the Dispersion of Windborne Material. *Meteor. Mag.* 90: 33–49.

Ratnam, M.V. and Basha, S.G. (2010). A robust Method to Determine Global Distribution of Atmospheric Boundary Layer top from COSMIC GPS RO Measurements. *Atmos. Sci. Lett.* 11: 216–222.

Seibert, P., Beyrich, F., Gryning, S.E., Joffre S., Rasmussen, A. and Tercier, P. (2000). Review and Intercomparison of Operational Methods for the Determination of the Mixing Height. *Atmos. Environ*. 34: 1001–1027.

Shi, B., Zheng, F. and Cao, G. (1997). On the Determination of Mixed Layer Height. *J. Xi'an Univ. Archit. Technol.* 29: 138–141.

Stevens, B. (2002). Entrainment in Stratocumulus Topped Mixed Layers. *Q. J. R. Meteorolog. Soc.* 128: 2663–2689.

Stull, R.B. (1988). *An Introduction to Boundary Layer Meteorology*, Kluwer Academic, The Netherlands.

Suarez, M.J., Arakawa, A. and Randall, D.A. (1983). The Parameterization of the Planetary Boundary Layer in the UCLA General Circulation Model: Formulation and Results. *Mon. Weather Rev.* 111: 2224–2243.

Tucker, S.C., Senff, C.J., Weickmann, A.M., Brewer, W.A., Banta, R.M., Sandberg, S.P., Law, D.C. and Hardesty, R.M. (2009). Doppler Lidar Estimation of Mixing Height Using Turbulence, Shear, and Aerosol Profiles. *J. Atmos. Oceanic Technol.* 26: 673–688.

van der Kamp, D. and McKendry, I. (2010). Diurnal and Seasonal Trends in Convective Mixed Layer Heights Estimated from Two Years of Continuous Ceilometer Observations in Vancouver BC. *Boundary Layer Meteorol.* 137: 459–475.

Wallace, L. (2000). Correlations of Personal Exposure to Particles with Outdoor Air Measurements: A Review of Recent Studies. *Aerosol Sci. Technol*. 32: 15–25.

Wesely, M.L., Cook, D.R., Hart, R.L. and Speer, R.E. (1985). Measurements and Parameterization of Particulate Sulfur Dry Deposition over Grass. *J. Geophys. Res.* 90: 2131–2143.

Yang, J., Li, X., Li, Q. and Wang, Z.W. (2011). Variation Characteristics of Atmospheric Stability and Mixed Layer Thickness and Their Relation to Air Pollution in Recent 30 Years in Urumqi. *Arid Land Geogr*. 34: 747–752.

Ye, D., Wang, F. and Chen, D. (2008). Multi-year Changes of Atmospheric Mixed Layer Thickness and Its Effect on Air Quality above Chongqing. *J. Meteorol. Environ.* 24: 41–44.

Received for review, October 8, 2012
Accepted, February 21, 2013